Gas-phase study on uridine: Conformation and X-ray photofragmentation

Eero Itälä,[1,a)] Kuno Kooser,[1] Elisabeth Rachlew,[2] Helena Levola,[1] Dang Trinh Ha,[1,3] and Edwin Kukk[1,4]
[1]*Department of Physics and Astronomy, University of Turku, FIN-20014 Turku, Finland*
[2]*Royal Institute of Technology KTH, Physics department, S-10691 Stockholm, Sweden*
[3]*Departamento de Química, Módulo 13, Universidad Autónoma de Madrid, 28049 Madrid, Spain*
[4]*Turku University Centre for Materials and Surfaces (MatSurf), FIN-20014 Turku, Finland*

(Received 23 December 2014; accepted 27 April 2015; published online 19 May 2015)

Fragmentation of RNA nucleoside uridine, induced by carbon 1s core ionization, has been studied. The measurements by combined electron and ion spectroscopy have been performed in gas phase utilizing synchrotron radiation. As uridine is a combination of d-ribose and uracil, which have been studied earlier with the same method, this study also considers the effect of chemical environment and the relevant functional groups. Furthermore, since in core ionization the initial core hole is always highly localized, charge migration prior to fragmentation has been studied here. This study also demonstrates the destructive nature of core ionization as in most cases the C 1s ionization of uridine leads to concerted explosions producing only small fragments with masses ≤43 amu. In addition to fragmentation patterns, we found out that upon evaporation the sugar part of the uridine molecule attains hexagonal form. © *2015 AIP Publishing LLC.* [http://dx.doi.org/10.1063/1.4919878]

I. INTRODUCTION

Ionizing radiation often causes irreversible damage when introduced into living tissue. The most sensitive parts of living cells are considered to be the DNA and RNA molecules and although the damage induced by radiation absorption takes place on the molecular level, it can lead to cell death or inactivation.[1] Ionization processes can be divided into valence and core ionization. Valence ionization dominates in the vacuum ultraviolet (VUV) range (~10-100 eV), whereas core ionization can only take place when the energy of the ionizing radiation is sufficient (generally >100 eV in lighter elements). In the case of lighter elements, core ionization is often followed by Auger decay leading to a doubly charged state.

Ionization-induced fragmentation of different biomolecules has been studied quite extensively using various techniques: ion- and electron bombardment,[2–6] electrospray ionization,[7,8] and photoionization[9–11] to name few. Gas phase studies have mostly concentrated on small free molecules, due to the difficulties in introducing larger molecules into the gas phase intact. These studies are essential if we want to understand the interaction of ionizing radiation and organic material on the molecular level. The single-molecule experiments serve also as benchmark for studies of more complex targets and help to explain how chemical environment, for example, influences the fragmentation induced by ionization. Our group has recently studied several DNA/RNA molecules in terms of core ionization.[12–15] Here, we report a fragmentation study on a core ionized nucleoside uridine and a combination of uracil and d-ribose. The applied experimental method is electron energy resolved photoelectron-photoion-photoion coincidence (PEPIPICO) spectroscopy,[16,17] which also allows the investigation of possible ionization site selective fragmentation effects. Since fragmentation of core ionized uracil and d-ribose has already been studied,[13,15] this study takes a step towards larger species in order to shed light on the matter of chemical environment's possible effects on fragmentation. This study is also closely related to earlier studies on fragmentation of uridine, 5-methyluridine and thymidine (a nucleoside formed of thymine and deoxy-d-ribose).[14,18]

Uridine is thermally quite unstable, although it can be introduced into gas phase intact by direct evaporation, great care must be taken when doing so.[18] This is likely one reason why there are so few publications concerning gas phase uridine. The ones, by Ptasińska *et al.*[19] and Rice *et al.*[20] have utilized inelastic electron scattering (by 70 eV electrons) providing information about fragmentation following valence ionization. This is also the case with the study of Levola *et al.*,[18] however they used 10 eV photons instead of electrons. Core ionization and its implications have thus not been studied so far. Because core ionization is also exactly what happens in the case of high energy (keV range) radiation-matter interactions, knowing the core ionization induced processes in free nucleosides could also give guidance on how the RNA/DNA strings fragment as a result of high energy radiation absorption such as medical X-rays.

II. EXPERIMENTAL

The apparatus and method for the present PEPIPICO measurements have already been described in detail in Ref. 21, and only a brief summary is given here. The apparatus consists of a modified Scienta SES-100 electron energy analyzer,[22] where the original CCD camera was replaced by a resistive anode detector (Quantar), and a home-made Wiley-McLaren type ion time-of-flight spectrometer with a 400 mm long ion drift tube. The ion spectrometer is equipped with 77 mm

a)Author to whom correspondence should be addressed. Electronic mail: ersita@utu.fi

Hamamatsu MCP detector. The ion detection electronics is based on a 1 GHz waveform digitizer card (Signatec PDA 1000). For the PEPIPICO measurements, the system is operated in pulsed extraction field mode and in the present experiment the extraction pulse voltage was ±100 V across the sample region, with the drift tube held at 465 V. According to the simulations of the ion TOF spectrometer under the given settings, ions with energies up to 2 eV have 2π collection efficiency that starts to gradually decrease at higher energies. The uridine samples were purchased from Sigma-Aldrich and all were used "as is" with their stated purities being 99%. The samples were evaporated into the interaction area using an effusion cell with integrated cooling shroud (MBE Komponenten NTEZ40 oven). The evaporation temperature was around 132 °C, which is below the thermal degradation temperature[18] and the pressure in the vacuum chamber during the measurement was $\sim 2 \times 10^{-7}$ millibars.

The PEPIPICO data always contain some false coincidences of particles not originating from the same molecule. The probability of such events was minimized by using low counting rates (<20 electrons/s). In addition, artificial coincidence events were created during the measurement by a pulse generator so that two electron-ion-ion coincidence maps were collected simultaneously—one in coincidence with electrons and one artificially triggered by the pulse generator. The average number of ions per electron trigger was 0.8 and the number of ions per artificial trigger 0.2 (including detector noise counts).

The experiment was performed at beamline I411 at the MAX-II synchrotron radiation facility (Lund, Sweden).[23] Undulator radiation was monochromatized using a modified Zeiss SX-700 monochromator. The ions were measured in coincidence with the C 1s photoelectrons at photon energy of 325 eV and using the electron kinetic energy detection window with range from 28 eV to 37 eV. The pass energy of the electron spectrometer was 100 eV and the entrance slit of the analyzer 1.6 mm, which corresponds to the energy resolution of about 750 meV. The electron energy scale in the PEPIPICO experiment was calibrated by measuring the CO 1s photoline at different center energy values of the electron detector keeping the photon energy at 325 eV. The center energy values were chosen so that the CO 1s photoline moved across the energy window by 1 eV steps. Using the measured electron hit coordinate values (x) of the peak maxima, a dispersion curve $E_k(x)$ was made. The shift correction of the binding energy scale for the electron spectrum of uridine was done by using the C 1s binding energy of CO.[24] The non-coincident photoelectron spectrum was measured using the constant pass energy mode, scanning the lens acceleration to cover the desired kinetic energy range. The slit and pass energy values were the same as for the coincidence measurements.

III. DISCUSSION

A. Ground state geometry of isolated uridine

Before attempting to disentangle the numerous fragmentation pathways, it is important to define the initial geometry of the molecule. Core-level photoelectron spectroscopy is suitable tool, as it probes the neutral state geometry of molecules as well as the changes caused by core ionization.[25] Uridine is traditionally assumed to have a geometry as presented in Fig. 1(a) and we do not question this if uridine is considered as a part of a larger system or in condensed phase.[26,27] Figure 2 shows the C 1s photoelectron spectrum of uridine measured with 325 eV photons together with the simulated spectra of the two geometries of Fig. 1. The spectra exhibit complex, highly convoluted structure due to the chemical shifts of the photolines from all together nine carbon atoms in different neighborhoods. The experimental spectrum was decomposed into individual peaks using the SPANCF curve-fitting package.[28,29] Reliable results can be obtained only by imposing strict constraints (i) all the peaks were fitted with a Voigt profile with equal, but adjustable Gaussian and Lorentzian width components. The fit resulted in 0.58 eV Gaussian and 0.52 Lorentzian full width at half-maximum (FWHM) values; (ii) all peaks were constrained to the same intensity, based on the assumption that the chemical environment does not affect the photoionization cross sections. The simulated spectra (with Gaussian and Lorentzian line widths of 0.50 eV) are based on the calculations described in the next paragraph.

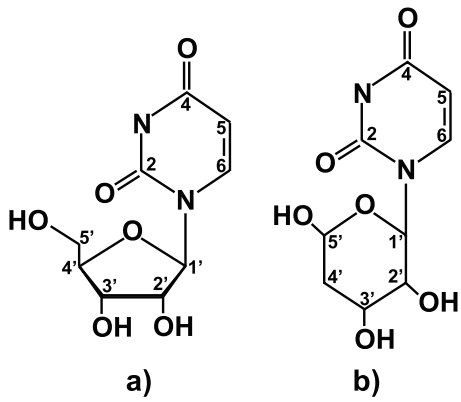

FIG. 1. Conformations of uridine ($C_9H_{12}N_2O_6$), where the sugar appears in furanose (a) and pyranose (b) forms.

The 1s binding energies of carbon atoms in various positions in the molecule were assigned to the peaks in the photoelectron spectrum based on relative molecular orbital energies calculated in the framework of Restricted Hartree-Fock theory[30] with the 6-311G(d,p) basis set.[31] The calculations were done by using the *ab initio* quantum chemistry code GAMESS.[32] The assignment of the photolines is approximated by using Koopman's theorem where the negative of the eigenvalue of an occupied orbital is equal to the ionization energy. The used split-valence triple-zeta basis set with added p- and d-type polarization functions is sufficiently flexible and appropriate for acquiring accurate geometries and relative energies of (at least) core molecular orbitals of the target molecule. The theoretical values are not absolute. The calculated photolines are presented in such a way that the C2's of both Geometries (a) and (b) of Fig. 1 are set at the same line for verification, for this reason two different shift values are used for the two geometries. This, consequently, may give an impression that C5 would be chemically more shifted than C2. In fact, the differences between the calculated binding energies of C atoms

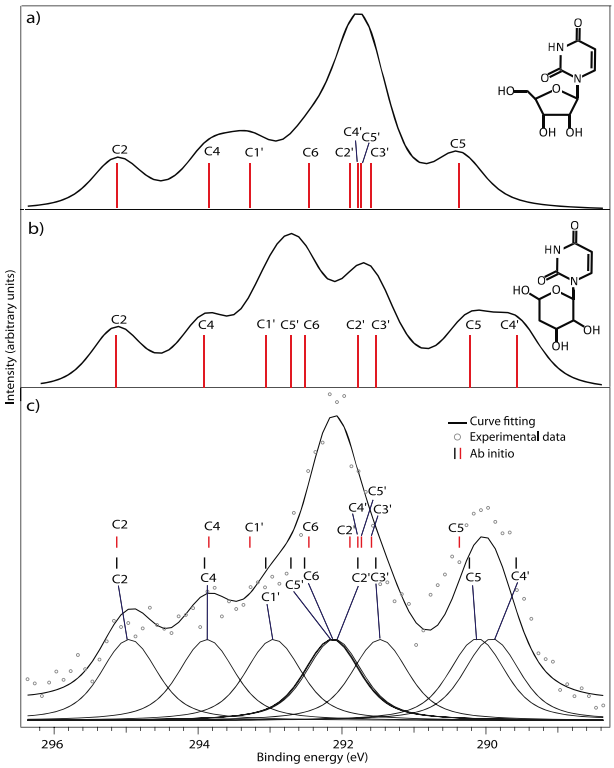

FIG. 2. Simulated spectra of uridine where the sugar is in furanose (a) and pyranose (b) forms together with the experimental C 1s photoelectron spectrum with curve fitting. The red and black bars in the experimental spectrum correspond to the theoretical assignments of the C 1s energies of individual carbon atoms of geometries (a) and (b) of Fig. 1, respectively (marked also in spectra (a) and (b)).

in the Uracil ring connected to the furanose and pyranose forms of the sugar are quite small—max. 245 meV (for the C2s) and min. 27 meV (for the C5s). The calculated C 1s photolines for the furanose geometry (a) of Fig. 1 are marked with red bars in Fig. 2(c), whereas the black bars correspond to the pyranose geometry (b) of Fig. 1.

At the high binding energy side, carbon C2 and C4, which are double-bonded to oxygen and have neighboring nitrogens, are well represented by the calculation for both geometries. In general, chemical shifts for the uracil carbons C1-C5 should be insensitive to the geometry change from furanose to pyranose form of the sugar, as is indeed shown by the calculations in Fig. 2. In contrast, the photolines of the sugar carbons C1'-C5' are very sensitive to the geometry change, particularly C4' showing a change in binding energy of 2.20 eV and C5' of 0.98 eV—these are the two carbons for which the nearest neighbors change. Regarding hydrogen bonding, Leulliot *et al.* determined that uridine has at least three stable conformers where the sugar part appears in furanose form and where there are hydrogen bonds between different hydrogen and oxygen atoms.[33] Our calculations show that the C 1s binding energies between different conformers are minimal at best and the effects of the hydrogen bonds are even smaller. The effect of the sugar moiety on the binding energies of the carbons in the uracil moiety is, however, noticeable. According to the results reported by Feyer *et al.*, the binding energies of the uracil moiety are few tenths of eV lower in uridine compared to free uracil.[34] For those carbons having higher binding energy, the decrease is smaller compared to those carbons with lower binding energy. For example, the binding energy difference in the case of C2 (the carbon with highest binding energy) is 0.4 eV whereas in the case of C5 (the carbon with lowest binding energy) the difference is 0.9 eV.

Let us now consider, how the calculation reproduces the experiment, concentrating on C4' and C5'. C4' is assigned, in the pyranose form (b), to the unresolved low binding energy structure (see Fig. 2(a)), but in the furanose form to the low binding energy shoulder of the dominant peak (see Fig. 2(b)). Moving one peak from the 290 eV structure to the 292 eV (while keeping equal intensities of peaks), one would not allow to obtain a good agreement of the fit with experiment. However, the furanose form (a) would also shift peak C5' from the higher binding energy side of the main structure to the lower one, which would, on the other hand, reduce the intensity distribution discrepancies. Therefore, it is quite unlikely, that the molecule is completely in the furanose form. Large fraction of the molecules have the pyranose structure, but a significant contribution from the furanose is possible and it would indeed improve the agreement between the modeled and the experimental spectra. The result is quite significant and is in line with Ref. 35, which concluded that evaporated sugar molecules are thermally more stable in the pyranose (hexagonal) form than in the furanose (pentagonal) form. It seems that the geometrical rearrangement towards preferable form is to take place even if a molecule (in this case d-ribose) is a part of a larger system. Furthermore, as the conformal rearrangement is activated by thermal energy, the energy required here is below the limit of thermal degradation.

B. Fragmentation patterns

The C 1s core ionization of uridine leads subsequently to Auger decay leaving the molecule at a highly unstable doubly charged state. In the case of uridine, this doubly charged state relaxes via fragmentation into two momentum-correlated cations and a number of neutral fragments. This is demonstrated by the PEPIPICO map presented in Figure 3, which represents each momentum-correlated ion pair as a slightly tilted elliptic pattern. An immediate observation is the low quality of the coincidence patterns in the map. This is not a result of experimental problems, but indicates that as one moves to larger and larger species, the coincidence quality decreases. The two main causes for this are that there is an abundance of fragment combinations and, every more importantly, that the presence of large neutral fragments often almost destroys the two-body momentum-correlation of the charged fragments. The latter problem is aggravated if the sites of origin of the charged fragments are well separated across the molecule. Despite the presence of heavy neutral fragments, the momentum-correlation of the charged fragments can still be retained in the case of sequential bond separations. The blurred shape of the patterns indicates that the fragmentation processes are not sequential, but rather single-step concerted explosions. The kinetic energy released in the charge separation process is thus not distributed between the charged fragments exclusively, but also the neutral species receive notable amount of energy. This was also observed with thymidine.[14]

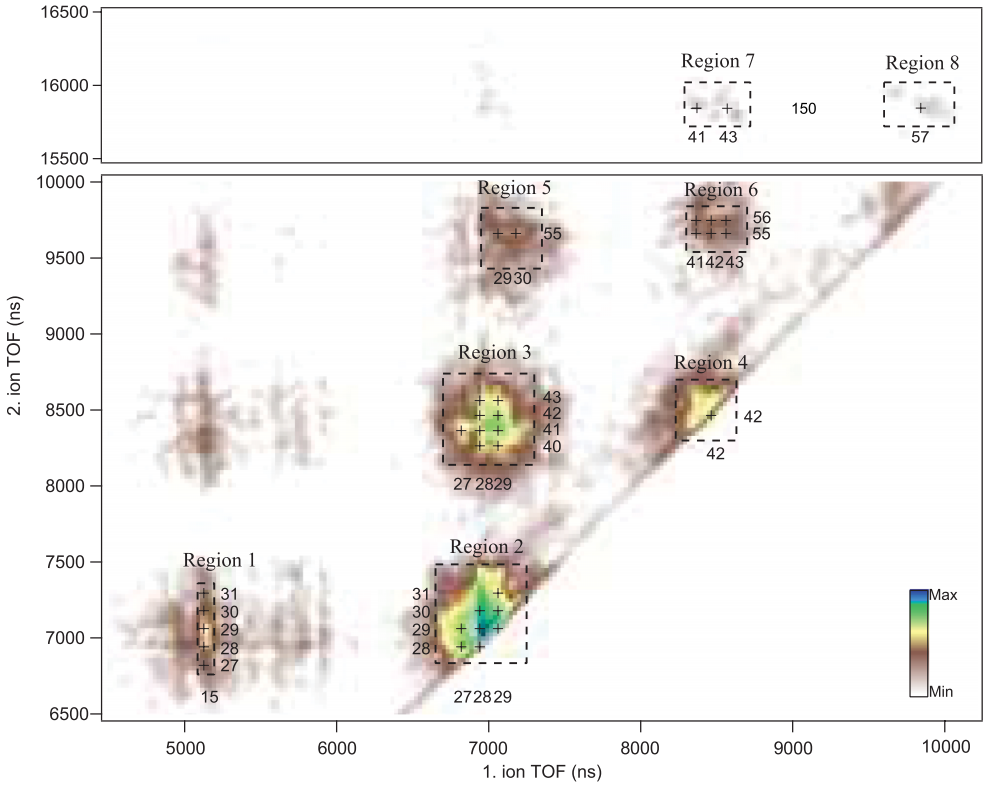

FIG. 3. PEPIPICO map of uridine. The center point of each PEPIPICO pattern corresponding to a coincident pair is marked with + and the numbers alongside the center coordinates of the PEPIPICO patterns are mass values (in amu). The bar on the right-down corner denotes the intensities of the patterns.

Table I sums up all the possible coincident fragment combinations; those considered less probable are in brackets. There are several fragments that cannot form by a simple bond cleavage process, but require protonation or hydrogen migration within the molecule. Such behavior is known to be common[36–38] and was also seen, for example, with thymidine and d-ribose.[14,15]

The smallest charged fragment of uridine corresponds to the mass 15 amu, which can be either CH_3^+ or NH^+. In the

TABLE I. Coincident cation pair combinations resulting from C 1s core ionization of uridine. The fragments considered to give minor contribution, if any, are in brackets.

M_1, M_2 (amu)	Fragment 1	Fragment 2	M_1, M_2 (amu)	Fragment 1	Fragment 2
15, 27	CH_3^+	CNH^+	28, 42	$HCNH^+$	NCO^+
	(NH^+)			(CO^+)	($C_2H_2O^+$)
15, 28	CH_3^+	$HCNH^+$	28, 43	$HCNH^+$	$HNCO^+$
	(NH^+)	(CO^+)		(CO^+)	($C_2H_3O^+$)
15, 29	CH_3^+	CHO^+	29, 40	CHO^+	C_2O^+
	(NH^+)		29, 41	CHO^+	C_2HO^+
15, 30	CH_3^+	CH_2O^+	29, 42	CHO^+	NCO^+
	(NH^+)				$C_2H_2O^+$
15, 31	CH_3^+	CH_3O^+	29, 43	CHO^+	$HNCO^+$
	(NH^+)				($C_2H_3O^+$)
27, 28	CNH^+	CO^+	42, 42	NCO^+	$C_2H_2O^+$
27, 29	CNH^+	CHO^+	29, 55	CHO^+	C_2HNO^+
28, 28	$HCNH^+$	CO^+	30, 55	CH_2O^+	C_2HNO^+
28, 29	$HCNH^+$	CHO^+	41, 55	C_2HO^+	C_2HNO^+
29, 29	CHO^+	CHO^+	42, 55	$C_2H_2O^+$	C_2HNO^+
29, 30	CHO^+	CH_2O^+	43, 55	$C_2H_3O^+$	C_2HNO^+
29, 31	CHO^+	CH_3O^+	41, 56	C_2HO^+	$C_2H_2NO^+$
28, 40	$HCNH^+$	C_2O^+	42, 56	$C_2H_2O^+$	$C_2H_2NO^+$
	(CO^+)		43, 56	$C_2H_3O^+$	$C_2H_2NO^+$
28, 41	$HCNH^+$	C_2HO^+	41, 150	C_2HO^+	$C_7H_6N_2O_2^+$
	(CO^+)		43, 150	$C_2H_3O^+$	$C_7H_6N_2O_2^+$
			57, 150	$C_2H_3NO^+$	$C_7H_6N_2O_2^+$

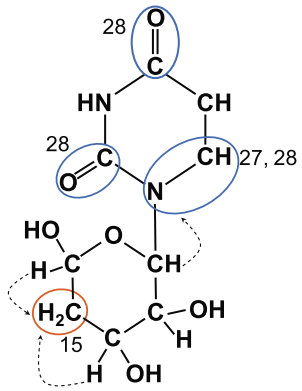

FIG. 4. Initial sites of CH_3^+, CHN^+, $HCNH^+$, and CO^+. The sites of CHO^+, CH_2O^+, and CH_3O^+ cannot be unambiguously determined and are thus not shown here. The dashed lines denote the most likely hydrogen migrations.

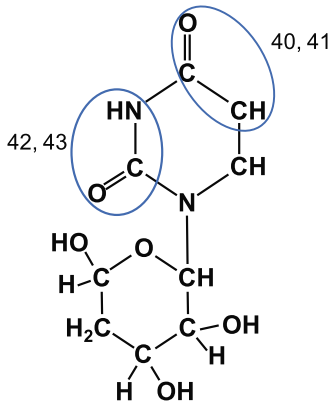

FIG. 5. Sites of origin of the 40-43 amu fragments when originating from the base.

case of core ionized d-ribose, only the CH_3^+ fragment was present, whereas in the case of uracil, neither CH_3^+ or NH^+ was detected.[13,15] Thus, although the formation of CH_3^+ requires either protonation, hydrogen migration, or both, it is likely that the fragment with mass 15 amu is CH_3^+ and originates from the sugar moiety (see Fig. 4). The CH_3^+ ion appears in coincidence with the 27-31 amu fragments (weak patterns inside region 1). These fragments are CHN^+, $HNCH^+/CO^+$ CHO^+, CH_2O^+, and CH_3O^+, respectively. The CHN^+ and $HCNH^+$ originate from the same site of the base (see Fig. 4); the formation of $HNCH^+$ is just accompanied by protonation/hydrogen migration to the CHN during the fragmentation process. Because in the case of uracil, the $HNCH^+$ was more abundant than CO^+,[13] we believe that this is also the case with uridine; we propose that CO^+ mainly appears in coincidence with $HNCH^+$ (and CHN^+, see next paragraph). CHO^+, CH_2O^+, and CH_3O^+ are all primarily located at the sugar part, where there are several possible initial sites for all these fragments.

Let us concentrate on the PEPIPICO patterns within region 2 of Fig. 3. From here on, we denote the coincident pairs with mass numbers only, *e.g.*, (28, 28). The CHN^+ (27 amu) appears in coincidence with CO^+ (28 amu) and CHO^+ (29 amu). The upper left corner of the (CHN^+, CHO^+) pair can be seen due to lack of the pattern (27, 30) (CHN^+, CH_2O^+). Those fragments in coincidence with $HNCH^+$ are a bit more difficult to identify due to the higher background level along the vertical line corresponding to 28 amu (~6950 ns). Our interpretation is that there are patterns corresponding to (28, 28-30), but the pattern (28, 31) originates from false coincidences not fully subtracted from the measurement data. The 28-30 amu ions in coincidence with $HNCH^+$ are CO^+ (from the base), CHO^+, and CH_2O^+ (both from the sugar part). The last patterns within region 2 are (29, 29) (CHO^+, CHO^+), (29, 30) (CHO^+, CH_2O^+), and (29, 31) (CHO^+, CH_3O^+). These coincident pairs are all originating purely from the sugar part of the uridine molecule, having several possible points of origin.

Region 3 represents the (27, 41), (28, 40-43), and (29, 40-43) patterns, where the 27, 28, and 29 amu fragments are CHN^+, $HNCH^+/(CO^+)$ (from the base as in Fig. 4), and COH^+ (from the sugar), respectively. The 40-43 amu fragments are assigned to C_2O^+, C_2HO^+, NCO^+ and $HNCO^+$, respectively. Such fragments were also found to be present in the case of core ionized uracil and thus the initial sites are designated as in Fig. 5. The 41-43 amu fragments with assignments of C_2HO^+, $C_2H_2O^+$, and $C_2H_3O^+$ can also come from the sugar part. For example, the only pattern inside region 4, the (42, 42) pattern, which can only correspond to (NCO^+ (from the base), $C_2H_2O^+$ (from the sugar)) pair, backs up this conclusion. However, based on the results concerning free thymidine or d-ribose,[14,15] we believe that only a small fraction of the 41-43 amu fragments' intensity is due to the C_2HO^+, $C_2H_2O^+$, and $C_2H_3O^+$ fragments coming from the sugar part.

There are also some weak patterns corresponding to heavier fragments (regions 5-8). Those with masses 55-56 amu originate from the base and are assigned to $C_2H_nNO^+$ (n = 1-2) with the initial site as in Fig. 6. The corresponding coincident fragments are presented in Table I; one should note that the 41-43 amu fragments within region 6 are, unlike in region 3, coming from the sugar part being C_2HO^+, $C_2H_2O^+$ and $C_2H_3O^+$. The heaviest fragment of core ionized uridine contains the whole base and a part of the sugar being that with the mass of 150 amu and assignment of $C_7H_6N_2O_2^+$ (see Fig. 7). It appears in coincidence with C_2HO^+, $C_2H_3O^+$ and $C_2HO_2^+$, which obviously must all come from the sugar part.

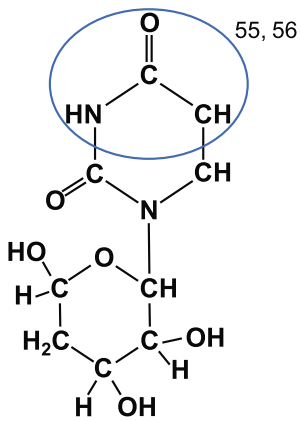

FIG. 6. Sites of origin of the 55 and 56 amu fragments ($C_2H_nNO^+$, n = 1-2).

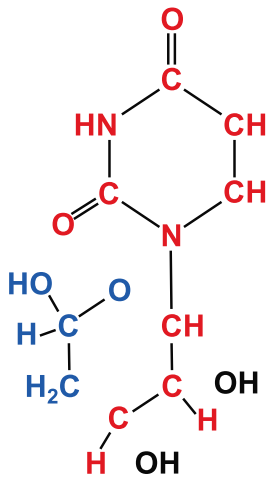

FIG. 7. $C_7H_6N_2O_2^+$ (red) contains the whole base and a part of the sugar moiety, the corresponding coincident ions (C_2HO^+, $C_2H_3O^+$, and $C_2HO_2^+$) come from the remaining part (blue).

C. Role of the chemical environment and the functional groups on fragmentation

The fragmentation of core ionized uridine cannot be described by the fragmentation of separated uracil and d-ribose dications; the sugar and the base contribute ionic fragments approximately equally and most of the ion pairs have initial sites in both the base and the sugar part of the uridine molecule. This study thus demonstrates (again) that although the initial core hole site is always located to either the sugar or the base, the valence final holes can relocate to a site far from the initial core hole. Here, for example, the glycosidic bond separating the sugar and the base moieties does not restrict such re-localization.

The fact that uridine is a combination of uracil and d-ribose provides an opportunity to investigate how chemical environment influences on the fragmentation of uracil and d-ribose. Although the C 1s core ionization of uridine results mainly to the same ion fragments as the C 1s core ionization of uracil and d-ribose, the coincident pairs are often not the same. Compared to thymidine, the relative contribution of coincident fragments originating purely from the sugar or the base is clearly lower in uridine. One reason could be that compared to thymidine, uridine has an additional -OH group in its sugar part. Levola *et al.* suggested that this causes the sugar part to be more fragile[18] which together with the fact that uracil has more fragmentation channels producing a high yield of coincident fragments than d-ribose, leads to the detected distribution of ion fragments. The larger variety of sugar-originated fragments in uridine than in thymidine and the existence of the large $C_7H_6N_2O_2^+$ is also believed to be connected to the extra -OH group; in the case of thymidine, no fragmentation channel producing a fragment containing a whole base existed.

D. Role of the initial ionization site on fragmentation

Because the PEPIPICO technique used in this work is electron-energy-resolved, it is possible to study whether the initial ionization site has an effect on fragmentation. In order to do this, the fragmentation patterns on the PEPIPICO map of Fig. 3 were divided into eight regions. The ion pair yields (PIPIYs) inside each region was then determined as a function of electron binding energy (*i.e.*, the initial ionization site) by

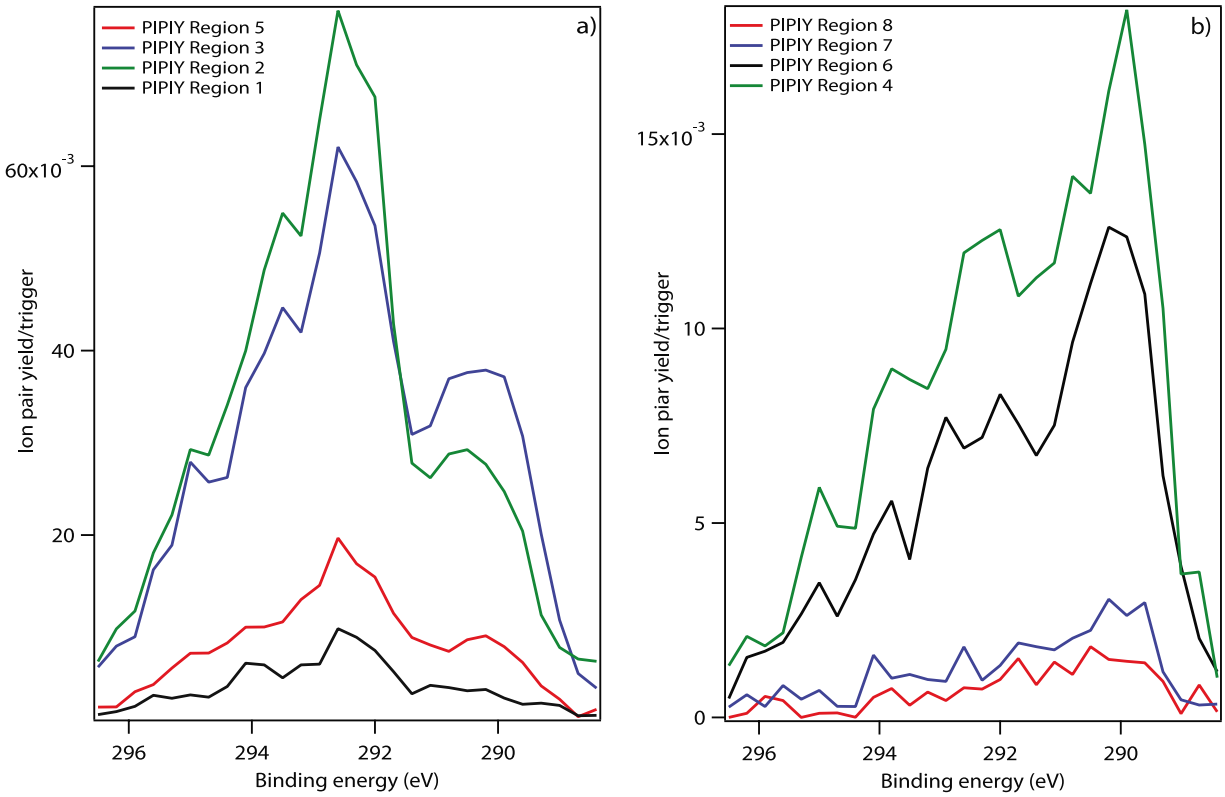

FIG. 8. Ion pair yields (PIPIYs) of the ions within regions 1, 2, 3, and 5 (a) and 4, 6, 7, and 8 (b) of the PEPIPICO map (Fig. 3).

counting the ion pairs within narrow (0.3 eV) ranges of electron energies. The resulting PIPIYs are presented in Figure 8 (note the different scales of ion pair yields). The PIPIYs corresponding to ion pairs within regions 2, 3, and 5 are clearly the highest, meaning that the corresponding fragmentation channels are also the dominant ones. As one can see, the shapes of these PIPIY curves have high resemblance to the photoelectron spectrum of Fig. 2(c). This indicates that the probability of these fragmentation channels do not depend on the initial ionization site. The PIPIY curves of regions 4 and 6, on the other hand, show a growing trend towards lower binding energy peaking at 290 eV. This means that the fragments inside regions 4 and 6 are preferably formed following the ionization of C5 and C4' (see Fig. 2(c)).

In neutral uridine, the valence orbitals are mainly delocalized over the whole molecule. However, there are few orbitals that are localized around the C5 or C'4 carbons. It is possible that the Auger decay preceding the formation of, for example, C_2HO^+ (the main fragment connected to a specific ionization site) involves electrons from these orbitals. The vacancies resulting from the Auger decay are thus effectively created when C5 and C4' 1s orbitals are ionized.

As a short summary, uridine does not exhibit any significant site specific fragmentation, dependence on the initial ionization site is only observed among the low-yield fragmentation channels. This behavior is very similar to the other cyclic molecules investigated by our group.[39]

IV. CONCLUSIONS

Fragmentation of uridine following site-selective core ionization and the subsequent Auger decay was studied with the help of the PEPIPICO technique. First, it was found that upon evaporation the uridine molecule easily changes its geometry from where the sugar part appears in the furanose (pentagonal) form into where the sugar appears in pyranose (hexagonal) form. Similarly to thymidine, the fragmentation pathways of the doubly charged uridine depend very little on the initial ionization site and are rather single-step concerted explosions than sequential many-step processes. Core ionization of uridine leads almost exclusively to the fragmentation into small fragments with masses ≤ 43 amu, with one usually originating from the base and the other from the sugar part of the molecule. The detected ion fragments often involve cleavage(s) of the bonds far from the initial ionization site. This suggests that the damage inflicted by the ionizing radiation is not restricted to the uracil or sugar moiety that initially absorbs the radiation, but can reach much further. This is similar to dissociative electron attachment in DNA; an electron captured by a nucleobase is often to cause strand breaks in the sugar-phosphate backbone, relatively far from the initial site where the electron capture takes place.[40,41]

The relative intensities of the individual ion fragments are quite the same in the case of uridine as in the cases of uracil and d-ribose and also same fragmentation channels exist. However, in uridine, the fragmentation channels of free uracil and d-ribose become often mixed and produce ion fragments from the sugar and the base in coincidence. The chemical environment, in the case of core ionization induced fragmentation of uracil and d-ribose in uridine, thus mainly affects the fragmentation channels (*i.e.*, the pairing of ions), not the bond cleavage sites. For comparison, in the case of core ionized thymidine, the coincident ions were mostly the same as in thymine and 2-deoxy-D-ribose, only the ratios between ion pairs were changed. So, although thymidine and uridine are very similar molecules (separated only by an -OH and a $-CH_3$ groups), combining the thymine and 2-deoxy-D-ribose into thymidine and uracil and d-ribose into uridine lead to quite different changes in fragmentation behavior. This indicates that the effects of the chemical environment cannot be easily predicted and the role of a simple functional group such as -OH is far from straightforward in the context of photofragmentation.

ACKNOWLEDGMENTS

Financial support from the Academy of Finland, the European COST Action XLIC CM1204 and the EU Transnational Access to Research Infrastructures programme. Computational resources from the FGI project (Finland) are acknowledged. D.T.H. acknowledges the Finnish Cultural Foundation for funding and the MINECO Project No. FIS2013-42002-R. E.R. acknowledges funding from the Swedish Research Council (VR). The authors thank the staff of MAX-lab for their help during the experiments and express their gratitude to the Electron Spectroscopy Group of the University of Oulu for the opportunity to share their experimental equipment.

[1]C. Von Sonntag and H. P. Schuchman, *Encyclopedia of Molecular Biology and Molecular Medicine* (VHC, Weinheim, 1996), Vol. 3.
[2]T. Fujií, Y. Inagaki, and Y. Mitsutsuka, Int. J. Mass Spectrom. Ion Processes **124**, 45 (1993).
[3]M. Vinodkumar, C. Limbachiya, M. Barot, M. Swadia, and A. Barot, Int. J. Mass Spectrom. **339-340**, 16 (2013).
[4]J. M. Rice, G. O. Dudek, and M. Barber, J. Am. Chem. Soc. **87**, 4569 (1965).
[5]M. Imhoff, Z. Deng, and M. A. Huels, Int. J. Mass Spectrom. **245**, 68 (2005).
[6]Z. Deng, I. Bald, E. Illenberger, and M. A. Huels, Phys. Rev. Lett. **95**, 153201 (2005).
[7]J. B. Fenn, M. Mann, C. K. Meng, S. F. Wong, and C. M. Whitehouse, Science **246**, 64 (1989).
[8]F. Rogalewicz, Y. Hoppilliard, and G. Ohanessian, Int. J. Mass Spectrom. **195-196**, 565 (2000).
[9]H.-W. Jochims, M. Schwell, H. Baumgärtel, and S. Leach, Chem. Phys. **314**, 263 (2005).
[10]M. Schwell, H.-W. Jochims, H. Baumgrtel, and S. Leach, Chem. Phys. **353**, 145 (2008).
[11]D. Touboul, F. Gaie-Levrel, G. Garcia-Macias, L. Nahon, L. Poisson, M. Schwell, and M. Hochlaf, J. Chem. Phys. **138**, 094203 (2013).
[12]E. Itälä, D. T. Ha, K. Kooser, E. Rachlew, M. A. Huels, and E. Kukk, J. Chem. Phys. **133**, 154316 (2010).
[13]E. Itälä, D. T. Ha, K. Kooser, E. Nõmmiste, U. Joost, and E. Kukk, Int. J. Mass Spectrom. **306**, 82 (2011).
[14]E. Itälä, M. A. Huels, E. Rachlew, K. Kooser, T. Hägerth, and E. Kukk, J. Phys. B: At., Mol. Opt. Phys. **46**, 215102 (2013).
[15]D. T. Ha, M. A. Huels, M. Huttula, S. Urpelainen, and E. Kukk, Phys. Rev. A **84**, 033419 (2011).
[16]J. H. D. Eland, F. S. Wort, and R. N. Royds, J. Electron Spectrosc. Relat. Phenom. **41**, 297 (1986).
[17]M. Simon, T. LeBrun, P. Morin, M. Lavolle, and J. L. Marchal, Nucl. Instrum. Methods Phys. Res., Sect. B **62**, 167 (1991).
[18]H. Levola, K. Kooser, E. Itälä, and E. Kukk, Int. J. Mass Spectrom. **370**, 96 (2014).
[19]S. Ptasińska, P. Candori, S. Denifl, S. Yoon, V. Grill, P. Scheier, and T. D. Märk, Chem. Phys. Lett. **409**, 270 (2005).
[20]J. M. Rice and G. O. Dudek, Biochem. Biophys. Res. Commun. **353**, 383 (1969).

[21]E. Kukk, R. Sankari, M. Huttula, A. Sankari, H. Aksela, and S. Aksela, J. Electron Spectrosc. Relat. Phenom. **155**, 141 (2007).
[22]M. Huttula, S. Heinäsmäki, H. Aksela, E. Kukk, and S. Aksela, J. Electron Spectrosc. Relat. Phenom. **156-158**, 270 (2007).
[23]M. Bässler, A. Ausmees, M. Jurvansuu, R. Feifel, J.-O. Forsell, P. de Tarso Fonseca, A. Kivimäki, S. Sundin, S. L. Sorensen, R. Nyholm, O. Björneholm, S. Aksela, and S. Svensson, Nucl. Instrum. Methods Phys. Res., Sect. A **469**, 382 (2001).
[24]V. Myrseth, J. D. Bozek, E. Kukk, L. J. Sæthre, and T. D. Thomas, J. Electron Spectrosc. Relat. Phenom. **122**, 57 (2002).
[25]K. Siegbahn, C. Nordling, A. Fahlman, R. Nordberg, K. Hamrin, J. Hedman, G. Johansson, T. Bergmark, S.-E. Karlsson, and I. Lindgren, *ESCA; Atomic, Molecular and Solid State Structure Studied by Means of Electron Spectroscopy*, Vetenskaps-Societeten i Upsala. Nova Acta; Ser. IV Vol. 20 (Almqvist & Wiksells, Uppsala, 1967).
[26]J. M. Neumann, J. M. Bernassau, M. Guéron, and S. Tran-Dinh, Eur. J. Biochem. **108**, 457 (1980).
[27]S. S. Ashraf, G. Ansari, R. Guenther, E. Sochacka, A. Malkiewicz, and P. F. Agris, RNA **5**, 503 (1999).
[28]E. Kukk, J. D. Bozek, G. Snell, W.-T. Cheng, and N. Berrah, Phys. Rev. A **63**, 062702 (2001).
[29]E. Kukk, K. Ueda, U. Hergenhahn, J. X. Liu, G. Prumper, H. Yoshida, Y. Tamenori, C. Makochekanwa, T. Tanaka, M. Kitajima, and H. Tanaka, Phys. Rev. Lett. **95**, 133001 (2005).
[30]C. C. J. Roothaan, Rev. Mod. Phys. **23**, 69-89 (1951).
[31]R. Krishnan, J. S. Binkley, R. Seeger, and J. A. Pople, J. Chem. Phys. **72**, 650 (1980).
[32]M. W. Schmidt, K. K. Baldridge, J. A. Boatz, S. T. Elbert, M. S. Gordon, J. H. Jensen, S. Koseki, N. Matsunaga, K. A. Nguyen, S. Su, T. L. Windus, M. Dupuis, and J. A. Montgomery, J. Comput. Chem. **14**, 1347 (1993).
[33]N. Leulliot, M. Ghomi, G. Scalmani, and G. Berthier, J. Phys. Chem. A **103**, 8716 (1999).
[34]V. Feyer, O. Plekan, R. Richter, M. Coreno, G. Vall-llosera, K. C. Prince, A. B. Trofimov, I. L. Zaytseva, T. E. Moskovskaya, E. V. Gromov, and J. Schirmer, J. Phys. Chem. A **113**, 5736 (2009).
[35]L. P. Guler, Y.-Q. Yu, and H. I. Kenttämaa, J. Phys. Chem. A **106**, 6754 (2002).
[36]D. Farcasiu, G. Miller, and C. S. Hsu, Org. Mass Spectrom. **25**, 409 (1990).
[37]E. Itälä, E. Kukk, D. T. Ha, S. Granroth, A. Caló, L. Partanen, H. Aksela, and S. Aksela, J. Chem. Phys. **131**, 114314 (2009).
[38]E. Itälä, K. Kooser, E. Rachlew, M. A. Huels, and E. Kukk, J. Chem. Phys. **140**, 234305 (2014).
[39]E. Itälä, D. T. Ha, K. Kooser, M. A. Huels, E. Rachlew, E. Nõmmiste, U. Joost, and E. Kukk, J. Electron Spectrosc. Relat. Phenom. **184**, 119 (2011).
[40]J. Gu, J. Wang, and J. Leszczynski, Nucleic Acids Res. **38**, 5280 (2010).
[41]X. Luo, Y. Zheng, and L. Sanche, J. Chem. Phys. **140**, 155101 (2014).